https://doi.org/10.15407/ujpe71.9.754

V.V. VYSHNEVSKYY,[1] I.A. PRYSHKO,[1] V.YO. STADNYK,[1] O.A. MARKEVYCH,[1] Z.O. KOHUT,[2,3] V.M. SALAPAK,[4] I.S. NOVOSAD[1]

[1] Ivan Franko Lviv National University
(6, Kyrylo and Mefodii Str., Lviv 79005, Ukraine; e-mail: Vasyl.Vyshnevskyi@lnu.edu.ua)
[2] National University "Lvivska Politechnika"
(12, Bandera Str., Lviv 79013, Ukraine)
[3] Czestochowa University of Technology
(Czestochowa, 42-201, Poland)
[4] Ukrainian National Forestry University
(103, General Chuprynka Str., Lviv, 79057, Ukraine)

PIEZOOPTIC EFFECT IN $LiRbSO_4$ CRYSTALS

An optically high-quality single crystal of $LiRbSO_4$ was synthesized, and the influence of uniaxial stress ($\sigma_m \approx 200$ bar) applied along various crystallophysical directions on the spectral (300–700 nm) and temperature (77–650 K) dependences of birefringence Δn_i was investigated. The results demonstrate that Δn_i is highly sensitive to uniaxial stress, exhibiting an almost linear increase with increasing pressure. The application of stress applied along different crystallographic directions leads to variations $\delta\Delta n_i$ that differ in both sign and magnitude. When a uniaxial stress of $\sigma_z = 77$ bar is applied, an optical pseudoisotropic point is induced in the crystal. The application of uniaxial stress does not alter the general shape of the $\Delta n_i(T)$ dependences; however, noticeable differences were observed in the magnitudes of the discontinuous changes in Δn_i at phase transitions, with the applied stress reducing the value of $\delta(\Delta n_i)$. The dispersion and temperature dependences of the piezooptic coefficients $\pi^0_{im}(\lambda)$ and $\pi^0_{im}(T)$ of $LiRbSO_4$ crystals were also examined. It was established that these coefficients exhibit weak dispersion, such that $\partial\pi^0_{im}/\partial T < 0$. The variations of $\pi^0_{im}(T)$ in the phase transition regions were analyzed in detail. The contributions of the electrooptic and elastoptic effects, as well as that of the order parameter, to the spontaneous changes in the piezooptic coefficients were evaluated. The analysis revealed that the largest contribution (approximately 80%) near the phase transition temperature T_4 is associated with the emergence of spontaneous polarization.

K e y w o r d s: crystal, birefringence, dispersion, uniaxial stress, phase transition, piezooptic coefficients.

1. Introduction

$LiRbSO_4$ (LRS) crystals possess a pseudohexagonal crystal structure and exhibit an unusual sequence of phase transitions (PTs): paraelectric phase I (symmetry $Pcmn$, $T_1 = 477$ K) $\rightarrow$ incommensurate phase II ($T_{c1} = 475$ K) $\rightarrow$ commensurate ferroelastic phase III ($P12_1/c1$, $T_3 = 458$ K) $\rightarrow$ ferroelectric phase IV ($P11n$, $T_4 = 439$ K) $\rightarrow$ paraelectric phase V ($P112_1/n$) [1, 2]. The incommensurate phase in LRS crystals was identified from the presence of satellite reflections in X-ray diffraction patterns and is characterized by a modulation wave vector [3, 4]. The complex sequence of phase transitions in LRS is associ-

C i t a t i o n: Vyshnevskyy V.V., Pryshko I.A., Stadnyk V.Yo., Markevych O.A., Kohut Z.O., Salapak V.M., Novosad I.S. Piezooptic effect in $LiRbSO_4$ crystals. *Ukr. J. Phys.* **71**, No. 9, 754 (2026). https://doi.org/10.15407/ujpe71.9.754.

ated with the structural modulation along the *c*-axis in the paraelectric phase I and the very small displacive distortion from the orthorhombic form in the low-temperature phases [5–7].

The dispersion dependences of the refractive indices $n_i(\lambda)$ at room temperature indicate that within the spectral range 250–850 nm, the dispersion is normal and increases sharply near the absorption edge [8–10]. Temperature measurements of $n_i(T)$ show that in phase I, the dependences are linear with slopes $dn_i/dT = (0.95\text{–}1.55) \times 10^{-5}$ K^{-1}. Upon transition to the incommensurate phase, pronounced temperature variations of the refractive indices were observed, with $dn_i/dT = (10.55\text{–}15.5) \times 10^{-5}$ K^{-1}. The PT at 458 K is accompanied by abrupt changes in $n_i(T)$, with $\delta n_i = (2.1\text{–}3.1) \times 10^{-4}$, which is indicative of a first-order transition [8–10]. A small thermal hysteresis of approximately 1.5 K was detected. The PT from phase IV to phase V is also a first-order transition, characterized by abrupt changes in $\delta n_i = (2.5\text{–}3.2) \times 10^{-4}$ and a hysteresis width of ∼3.5 K.

Using the temperature dependences of the refractive indices $n_i(T)$, the corresponding temperature variations of the electronic polarizabilities $\alpha_i(T)$ were calculated. It was established that $\alpha_i(T)$ decreases with decreasing temperature. Upon transition to the incommensurate phase, a slight inflection of the $\alpha_i(T)$ curves is observed. The most significant changes occur at the PT temperature of 439 K, where $\Delta\alpha_i = (4\text{–}8) \times 10^{-25}$ cm^3. In phase V, $\alpha_i(T)$ decreases almost linearly with temperature in all principal optical directions.

Despite the detailed studies of the spectral and temperature variations of the refractive parameters of LRS crystals, their piezooptic coefficients have not been investigated to date. The study of piezooptic coefficients is of both fundamental and applied interest, as it provides insight into one of the key crystal-optical parameters and enables an analysis of the temperature and spectral dependences of the deformation of the optical indicatrix under mechanical stress [11–18].

The piezooptic effect describes the change in the optical properties of a material (refractive index (n), birefringence (Δn), and dielectric permittivity (ε) at optical frequencies) under the influence of mechanical stress (σ_m). This effect is most conveniently expressed in terms of the induced changes in the polarization constants $a_{ij} = 1/n_{ij}^2 = 1/\varepsilon_{ij}$ [11, 12]. The tensor representation of the piezooptic and elastooptic effects has the following form: $\Delta\alpha_{ij} = \pi_{ijkl}\sigma_{kl}$ and $\Delta\alpha_{ij} = p_{ijkl}\chi_{kl}$. Here, $\Delta\alpha_{ij}$ is the change in the polarization constant, π_{ijkl} is the fourth-rank piezooptic tensor, p_{ijkl} is the fourth-rank elastooptic tensor, σ_{kl} is the second-rank mechanical stress tensor, and χ_{kl} is the second-rank strain tensor.

Particular attention should be paid to the behavior of the piezooptic coefficients in the vicinity of phase transitions between the paraelectric (PE), incommensurate (IC), and commensurate (C) phases. Previous studies have reported pronounced anomalies only near the ferroelectric (FE) phase transition, where the magnitudes of the coefficients may exceed their values in the FE or PE phases by one to two orders of magnitude [19–21].

In the present work, we report the results of a comprehensive study of both combined and absolute piezooptic coefficients of $LiRbSO_4$ crystals over a wide spectral and temperature range encompassing the phase-transition regions and optical isotropic points.

2. Experimental Procedure

The lithium–rubidium sulfate crystals investigated in this work were grown from an aqueous solution by the slow evaporation of the solvent under controlled conditions, including a constant growth temperature t_p, supersaturation degree δ, solution pH, and hydrostatic pressure [22]. Chemically pure lithium sulfate (Li_2SO_4) and rubidium sulfate (Rb_2SO_4) salts were used as starting reagents in a stoichiometric molar ratio:

$$Li_2SO_4 + Rb_2SO_4 + H_2O \rightarrow 2LiRbSO_4 + H_2O. \quad (1)$$

The components were repeatedly recrystallized prior to use to ensure high purity. $LiRbSO_4$ crystals were grown at a temperature of 318 K, with an average growth rate of (0.1 ± 0.05) mm/day. The temperature was maintained using a thermostat with an accuracy of ±0.5 K. Over a period of 30–40 days, optically homogeneous and transparent $LiRbSO_4$ crystals were obtained in the form of hexagonal plates with a volume of approximately 3–6 cm^3. A photograph of a typical grown crystal is shown in Fig. 1. Crystal orientation was determined by the extinction methods under a polarizing microscope and by analyzing conoscopic figures. Orientation was established according

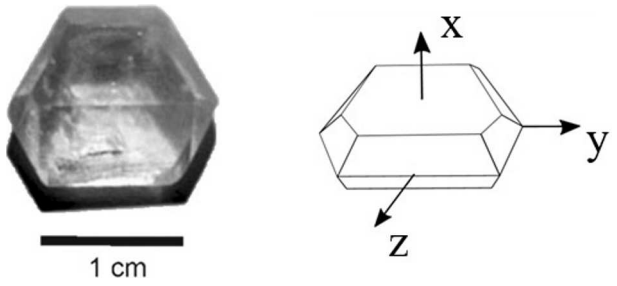

Fig. 1. Appearance and crystallographic orientation of $LiRbSO_4$ crystal grown by the evaporation method

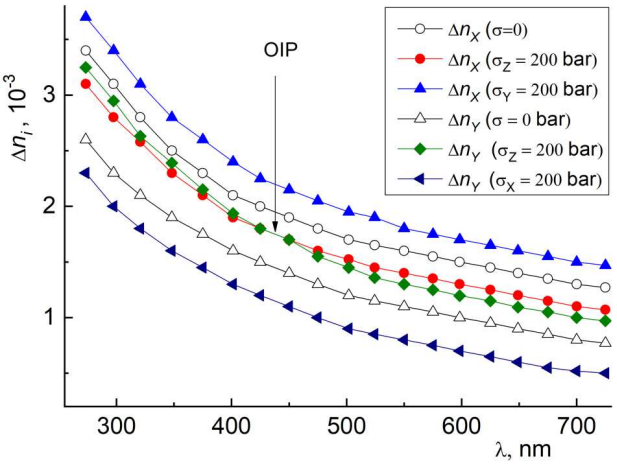

Fig. 2. Dispersion of birefringence in $LiRbSO_4$ crystals at room temperature for different directions of compression: light symbols – stress-free crystal, dark symbols – crystal under mechanical stress $\sigma_m = 200$ bar. OIP – optical isotropic point

to the space group $P112_1/n$ in the paraelectric phase, characterized by the lattice parameters $b < c < a$.

In this work, a polarization-optical method was used to determine the piezoelectric constants. This method involves passing light through a system consisting of a crossed polarizer and analyzer, with the crystal placed between them in a diagonal orientation. In the focal plane of the DFS-8 diffraction spectrograph, an interference pattern was observed, consisting of a series of maxima and minima [22, 23], whose intensity was determined by the following relationship:

$$I = I_0 \sin^2\left(\frac{\pi d}{\lambda}\Delta n_i\right), \tag{2}$$

where I is the intensity of transmitted light, I_0 is the incident light intensity, d is the thickness of the crystal along the light path, λ is the wavelength of light, and Δn_i is the birefringence induced in the crystal due to piezoelectric deformation.

When a mechanical stress σ_m is applied to the crystal, a shift in the interference pattern is observed. If a maximum shifts to the position of a minimum, or vice versa, then σ_m corresponds to the half-wave stress σ_{km}, and the piezoelectric coefficient can be determined from the relation:

$$\pi^0_{im} = 2\frac{\delta(\Delta n_i d_i)}{\sigma_m d_i} = \frac{\lambda}{\sigma^0_{im}}. \tag{3}$$

If the half-wave stress cannot be attained experimentally, it can be determined by interpolation using the following relation:

$$\sigma_{im} = \frac{\sigma_m \Delta\lambda}{\Delta\lambda'}, \tag{4}$$

where $\Delta\lambda$ is the wavelength interval between a minimum and a maximum of the interference pattern, and $\Delta\lambda'$ is the wavelength interval corresponding to the shift toward the minimum. By determining the magnitude and direction of the shifts of interference minima, the magnitude and sign of the induced birefringence can be unambiguously evaluated.

3. Results and Discussion

3.1. Pressure-induced changes of birefringence in $LiRbSO_4$ crystals

Figure 2 shows the dispersion of the birefringence $\Delta n_i(\lambda)$ of $LiRbSO_4$ crystals at room temperature for different directions of compression. It can be seen that the dispersion $\Delta n_i(\lambda)$ is normal across the investigated spectral range, with the relation $|d\Delta n_z/d\lambda| > |d\Delta n_x/d\lambda| > |d\Delta n_y/d\lambda|$. The observed behavior of the $\Delta n_i(\lambda)$ dispersion confirms the absence of optical isotropic points in this crystal.

However, from Fig. 2, it is evident that the $\Delta n_x(\lambda)$ and $\Delta n_y(\lambda)$ curves under a load of $\sigma_z = 200$ bar intersect at a wavelength of $\lambda \approx 423$ nm, corresponding to the emergence of a new optical "pseudo-isotropic" state. With increasing pressure, this point shifts towards shorter wavelengths at a rate of $\frac{d\lambda_0}{d\sigma} = 0.51$ nm $\cdot$ bar^{-1}, which is consistent with the pressure-induced change in the isotropic state in the isomorphic $LiKSO_4$ crystal under σ_z [24, 25]. In $LiKSO_4$, the stress σ_y shifts the isotropic point towards the long-wavelength region at a rate of $\frac{d\lambda_0}{d\sigma} =$

$= 4.8 \times 10^{-2}$ nm · bar^{-1}, while the pressure σ_z shifts it to the short-wavelength region at a rate of $\frac{d\lambda_0}{d\sigma} = -3.4 \times 10^{-2}$ nm · bar^{-1}.

Overall, it was established that the birefringence Δn_i of $LiRbSO_4$ is highly sensitive to uniaxial stresses and increases almost linearly with increasing applied pressure:

$$\delta(\Delta n_x) = +4.2 \times 10^{-4} \text{ and } -2.6 \times 10^{-4},$$
$$(\sigma_y = 200 \text{ bar and } \sigma_z = 200 \text{ bar}),$$
$$\delta(\Delta n_y) = +2.3 \times 10^{-4} \text{ and } -1.4 \times 10^{-4},$$
$$(\sigma_z \text{ and } \sigma_x = 200 \text{ bar}),$$
$$\delta(\Delta n_z) = +4.9 \times 10^{-4} \text{ and } -2.7 \times 10^{-4},$$
$$(\sigma_x \text{ and } \sigma_y = 200 \text{ bar}).$$

As can be seen from the figure, under uniaxial pressure applied along the Z-direction, Δn_x decreases while Δn_y increases, and at $\sigma_z = 77$ bar they become equal, $\Delta n_x = \Delta n_y = 1.11 \times 10^{-3}$. Under these experimental conditions, the optical indicatrix is thus characterized by two birefringence values, indicating an increase in its symmetry. It can be assumed that at this pressure an optically pseudoisotropic point is induced in the $LiRbSO_4$ crystal..

In general, an optically biaxial crystal is characterized by three principal values of Δn_i, whereas an optically uniaxial crystal has only one value of Δn_i. For $LiRbSO_4$, the following relation holds: $n_y > n_z > n_x$. The equality $\Delta n_x = \Delta n_y$ occurs when $n_y - n_z = n_z - n_x$, or equivalently, $n_x + n_y = 2n_z$. A similar situation was previously observed for a number of other isomorphic crystals of the $ABSO_4$ group [26–28], where equality of Δn_i occurred under σ_m applied along different crystallographic directions.

Overall, uniaxial mechanical stresses, while altering the magnitude of Δn_i, do not significantly change the character of the birefringence dispersion: $d\Delta n_x/d\lambda = 1.56 \times 10^{-6}$ and 1.54×10^{-6} nm^{-1} (σ_z and $\sigma_y = 200$ bar), and $d\Delta n_y/d\lambda = 1.59 \times 10^{-6}$ and 1.62×10^{-6} nm^{-1} (σ_z and $\sigma_x = 200$ bar).

According to Eq. (4), the corresponding pressure-induced changes in Δn_i can be expressed as follows:

$$\delta(\Delta n_x^z) \approx \frac{1}{2}\left(n_z^3\pi_{33} - n_y^3\pi_{23}\right),$$
$$\delta(\Delta n_y^z) \approx \frac{1}{2}\left(n_z^3\pi_{33} - n_x^3\pi_{13}\right). \quad (5)$$

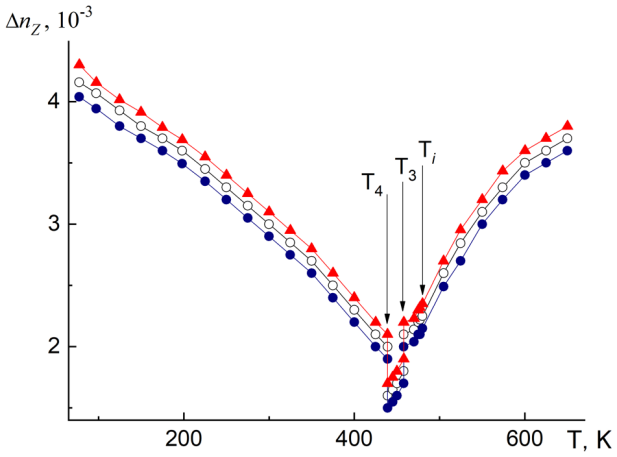

Fig. 3. Temperature dependences of the birefringence Δn_Z of the $LiRbSO_4$ crystal at $\lambda = 500$ nm (light symbols – stress-free crystal; red and blue symbols – uniaxially stressed crystals with $\sigma_X = 200$ bar and $\sigma_Y = 200$ bar, respectively)

Thus, the following relation between the refractive indices and the absolute piezoelectric coefficients near the OIP can be obtained:

$$n_y^3\pi_{23} \approx n_x^3\pi_{13}. \quad (6)$$

Since at $\lambda = 500$ nm the values $n_y = 1.4860$ and $n_x = 1.4834$ are close, the corresponding piezoelectric coefficients will also be close in absolute value.

Figure 3 shows the temperature dependences of Δn_z for stress-free and uniaxially stressed crystals ($\sigma_x = 200$ bar and $\sigma_y = 200$ bar). It was found that in the high-temperature phase I, the $\Delta n_i(T)$ dependences are almost linear for the X- and Y-directions:

$$\frac{d\Delta n_y}{dT} = 2.3 \times 10^{-6} \text{ K}^{-1},$$
$$\frac{d\Delta n_x}{dT} = 2.3 \times 10^{-6} \text{ K}^{-1}.$$

In the Z-direction, the birefringence varies nonlinearly – with increasing temperature, Δn_z tends to saturation. The transition to the incommensurate phase is accompanied by a change in the slope of the $\Delta n_i(T)$ curves, with a significant temperature-induced variation in birefringence being observed in the incommensurate phase:

$$\frac{d\Delta n_x}{dT} = 7.4 \times 10^{-5} \text{ K}^{-1},$$
$$\frac{d\Delta n_y}{dT} = 14.8 \times 10^{-5} \text{ K}^{-1},$$
$$\frac{d\Delta n_z}{dT} = 13.0 \times 10^{-5} \text{ K}^{-1}.$$

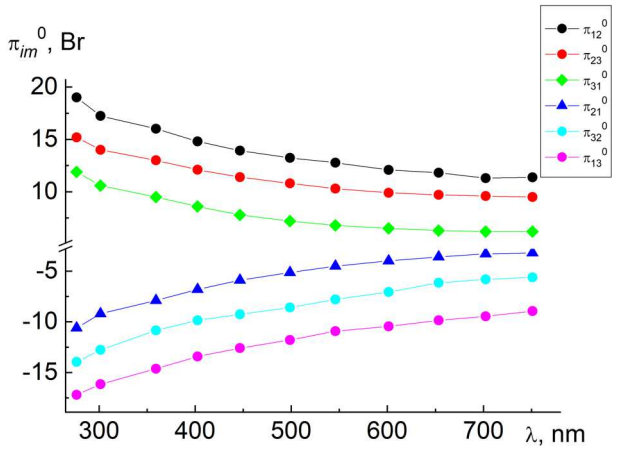

Fig. 4. Dispersion dependences of piezo-optical coefficients $\pi_{im}^0(\lambda)$ of $LiRbSO_4$ crystals at room temperature

In the Z-direction – the direction of incommensurate modulation – the largest changes in birefringence were observed. The ferroelectric–paraelectric (FE–PE) transition at 458 K is accompanied by an abrupt decrease in Δn_i:

$$\delta(\Delta n_x) = -1.4 \times 10^{-4},$$
$$\delta(\Delta n_y) = -1.5 \times 10^{-4},$$
$$\delta(\Delta n_z) = -1.8 \times 10^{-4}.$$

Further cooling leads to a more rapid decrease in Δn_i:

$$\frac{d\Delta n_x}{dT} = 14.4 \times 10^{-5}\ \mathrm{K}^{-1},$$
$$\frac{d\Delta n_y}{dT} = 18.5 \times 10^{-5}\ \mathrm{K}^{-1},$$
$$\frac{d\Delta n_z}{dT} = 17.4 \times 10^{-5}\ \mathrm{K}^{-1}.$$

The transition to the paraelectric phase at 439 K is accompanied by an abrupt increase in Δn_i:

$$\delta(\Delta n_x) = +2.5 \times 10^{-4},$$
$$\delta(\Delta n_y) = +2.9 \times 10^{-4},$$
$$\delta(\Delta n_z) = +3.6 \times 10^{-4}.$$

In the paraelectric phase V, Δn_i increases almost nonlinearly upon cooling, with average coefficients:

$$\frac{d\Delta n_x}{dT} = -4.4 \times 10^{-6}\ \mathrm{K}^{-1},$$
$$\frac{d\Delta n_y}{dT} = -2.2 \times 10^{-6}\ \mathrm{K}^{-1},$$
$$\frac{d\Delta n_z}{dT} = -6.5 \times 10^{-6}\ \mathrm{K}^{-1}.$$

Application of uniaxial stress does not change the overall character of the $\Delta n_i(T)$ dependences. Differences are observed only in the magnitudes of the temperature coefficients $d\Delta n_i/dT$. For example, in paraelectric phase V, upon cooling, Δn_i increases with the following average coefficients:

$$\frac{d\Delta n_z}{dT} = -6.8 \times 10^{-6}\ \mathrm{K}^{-1},$$
$$\frac{d\Delta n_z}{dT} = -6.1 \times 10^{-6}\ \mathrm{K}^{-1},$$

for stresses $\sigma_X = 200$ bar and $\sigma_Y = 200$ bar, respectively.

Differences were also found in the magnitudes of the jump-like changes in Δn_i during the FE–PE transition to the paraelectric phase V. For stresses $\sigma_m = 200$ bar, the jumps are:

$$\delta(\Delta n_x) = +2.2 \times 10^{-4},$$
$$\delta(\Delta n_y) = +2.7 \times 10^{-4},$$
$$\delta(\Delta n_z) = +3.3 \times 10^{-4}.$$

During the FE transition at $T_3 = 458$ K, the following decreases in Δn_i were observed:

$$\delta(\Delta n_x) = -1.1 \times 10^{-4},$$
$$\delta(\Delta n_y) = -1.2 \times 10^{-4},$$
$$\delta(\Delta n_z) = -1.5 \times 10^{-4}.$$

3.2. Pressure-induced changes in birefringence in $LiRbSO_4$ crystals

Figure 4 presents the dispersion dependences of the piezooptic coefficients $\pi_{im}^0(\lambda)$ of $LiRbSO_4$ crystals at room temperature. As can be seen, within the investigated spectral range, the piezooptic constants of the LRS crystal exhibit only a slight dispersion. Moreover, the nature of their dispersion mirrors that of the birefringence dispersion $\partial\pi_{im}^0/\partial\lambda < 0$. The most pronounced wavelength-dependent variations are observed for the coefficients π_{12}^0 and π_{13}^0, which correspond to the changes in Δn_x under the influence of the stresses σ_z and σ_y, respectively ($\partial\pi_{12}^0/\partial\lambda \approx \approx \partial\pi_{13}^0/\partial\lambda \approx 1.6 \times 10^{-2}$ Br/nm).

Figure 5 illustrates the temperature dependences of the piezooptic coefficients of $LiRbSO_4$ crystals at $\lambda = 500$ nm. In phase I, all coefficients π_{im}^0 slightly

decrease in absolute value with increasing temperature $\left|\frac{d\pi^0_{im}}{dT}\right| \approx 5.3 \times 10^{-3}$ Br $\cdot$ K^{-1}. The phase transition (PT) to phase II is accompanied by an abrupt reduction in the piezooptic coefficients of approximately $|\delta\pi^0_{im}| \approx 1.20$ Br on average. The largest variations are observed for the coefficients π^0_{31} and π^0_{32} ($\delta\pi^0_{31} = -1.41, \delta\pi^0_{32} = 1.38$ Br). It is known [29–32] that in crystals of the A_2BX_4 family, which undergo a sequence of phase transitions (paraelectric $\rightarrow$ incommensurate $\rightarrow$ ferroelectric $\rightarrow$ ferroelectric phase), the piezooptic effect is determined by both "intrinsic" and "secondary" contributions. In general, variations in the piezooptic coefficients can be described as the sum of the intrinsic piezooptic effect and the secondary effects:

$$\pi^0_{im} = 2\frac{d\Delta n_k}{d\sigma_m} = 2\left[\left(\frac{d\Delta n_k}{d\sigma_m}\right)_{i\ \mathrm{cm}} + \frac{d\Delta n_k}{dP_c}\frac{dP_c}{d\sigma_m} + \right.$$

$$\left. + \frac{d\Delta n_k}{d\chi^s}\frac{d\chi^s}{d\sigma_m} + \frac{d\Delta n_k}{d(\omega\rho^2)}\frac{d(\omega\rho^2)}{d\sigma_m}\right]. \qquad (7)$$

Here, the first term corresponds to the "true" piezo-optic effect, whereas the following terms describe the secondary contributions arising from the spontaneous polarization ($d\Delta n_k/dP_c$), spontaneous strain ($d\Delta n_k/d\chi^s$), and the order parameter ($d\Delta n_k/d(\omega\rho^2)$).

The electrooptic contribution originates from the temperature dependence of the spontaneous polarization P_s and the shift of the $P_s(T)$ function along the temperature axis under uniaxial stress σ_m. As a result, P_s changes by an amount δP_s, which leads to an additional electrooptic modification of the birefringence. To estimate the contribution of the electrooptic effect, one should use the dependence $P_s(T)$ [1, 2] and the experimental data for the baric shift of the phase transition point $dT_c/d\sigma_m$ [10]. The spontaneous polarization of $LiRbSO_4$ is relatively small (maximum $P_s \approx$ ≈ 10 mC/cm^2), while the baric shift of the PT is $dT_4/d\sigma_m \approx 0.017$ K/bar. Assuming that the shape of the $P_s(T)$ curve remains unchanged under σ_m, one can estimate the electrooptic contribution to the variation of the piezooptic coefficients near the PT. Our results show that this contribution is maximal near the PT (~80%) and decreases to about 10–15% further into the ferroelectric phase. These values agree well with the differences between the coefficients π^0_{31} measured in the ferroelectric phase and those extrapolated from the paraelectric phase (Fig. 6).

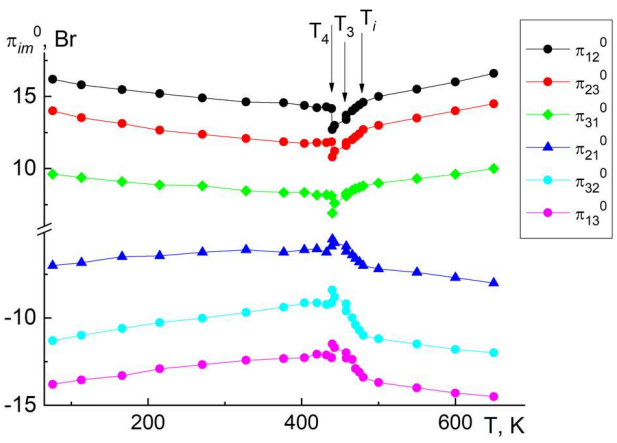

Fig. 5. Temperature dependences of piezooptic coefficients $\pi^0_{im}(T)$ of $LiRbSO_4$ crystals for wavelength of light $\lambda = 500$ nm

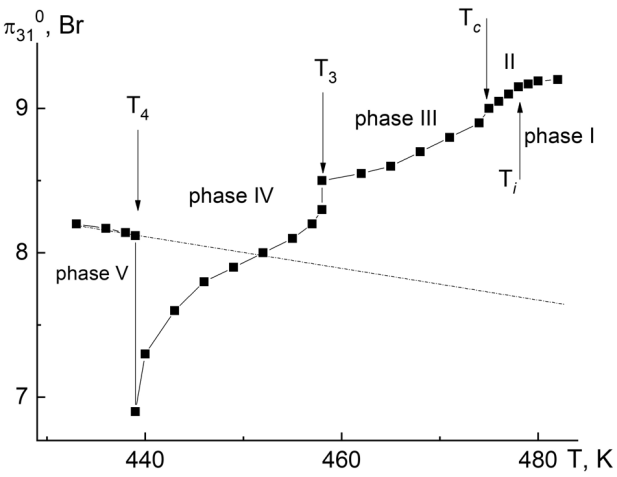

Fig. 6. Temperature dependences of piezooptic coefficients π^0_{31} of $LiRbSO_4$ crystals at region of phase transitions

In phase IV, the piezooptic coefficients first increase rapidly (for example, $\frac{d\pi^0_{31}}{dT} = 0.16$ Br/K), and then the growth rate decreases ($\frac{d\pi^0_{31}}{dT} = 0.04$ Br/K). The PT to phase III is accompanied by a slight increase of approximately $|\delta\pi^0_{im}| \approx 0.2$ Br. Since phase III is ferroelectric, this anomaly results from the emergence of spontaneous strain χ_s. Thus, the piezooptic effect in this phase is governed by both the intrinsic contribution and secondary electrooptic and elastoptic effects $d\Delta n_i/d\chi_s$.

The elastooptic contribution arises from the temperature dependence of the spontaneous strain χ_s and the shift of the $\chi_s(T)$ curve along the temperature axis under uniaxial stress σ_m. Consequently, χ_s changes by $\delta\chi_s$, causing an additional elastooptic change in birefringence. Although the $\chi_s(T)$ dependence is not available in the literature, this contribution can be estimated from the difference between the coefficients π^0_{31} in the ferroelectric and ferroelastic phases (Fig. 4) and amounts to approximately 85%.

Further heating leads to a slight increase in the piezooptic coefficients $\frac{d\pi^0_{im}}{dT} \approx 0.03$ Br/K.

The PT to the incommensurate phase is accompanied by a change in the slope of the temperature dependence of the piezooptic coefficients, $\frac{d\pi^0_{im}}{dT} \approx 0.07$–0.09 Br/K.

The observed anomalies can be interpreted as follows. Crystals with incommensurate structures are characterized by the emergence of a modulated superstructure within a certain temperature range between the ordered and disordered base phases. This superstructure has a period incommensurate with that of the crystal lattice. Such structures exhibit a soliton structure characterized by the soliton density $n_s(\omega\rho^2)$, which acts as the order parameter. This parameter reaches its maximum near T_i and vanishes abruptly near T_c.

Therefore, the total piezooptic effect in the incommensurate phase is determined by the intrinsic and secondary contributions, the latter being primarily governed by the order parameters in the piezooptic coefficients π^0_{im}. By linearly extrapolating the temperature dependences $\pi^0_{31}(T)$ from the paraelectric phase into the region below $T_i = 475$ K, the variations in the coefficients in the incommensurate and commensurate phases caused by the order parameter and spontaneous polarization can be derived.

The respective contributions from spontaneous polarization (electrooptic effect), spontaneous strain (elastooptic effect), and the order parameter to the spontaneous variation in the piezooptic coefficient $\Delta\pi$ were analyzed. It was found that in the incommensurate phase, upon cooling, the contribution of the order parameter increases up to 65%, while that of the spontaneous strain decreases to about 35%.

At 477 K, the crystal transforms into the paraelectric phase, accompanied by a slight increase in the piezooptic coefficients $\pi^0_{im}(T)$. However, the temperature variations become significantly smaller than in the incommensurate phase, $\frac{d\pi^0_{im}}{dT} \approx \approx 0.02$–$0.04$ Br/K.

4. Conclusions

In this work, an optically high-quality $LiRbSO_4$ crystal was synthesized, and the influence of uniaxial stress $\sigma_m \approx 200$ bar along different crystallophysic directions on the spectral (300–700 nm) and temperature (77–650 K) dependences of birefringence Δn_i was investigated. It was found that Δn_i is highly sensitive to uniaxial stress and increases almost linearly with pressure. Moreover, applying stress along different crystallophysic directions leads to changes $\delta\Delta n_i$ with different magnitudes and signs.

Under uniaxial stress $\sigma_z = 77$ bar, the birefringence components Δn_x and Δn_y become equal, $\Delta n_x = \Delta n_y = 1.11 \times 10^{-3}$, indicating increased symmetry of the optical indicatrix and, consequently, the emergence of an optical pseudoisotropic point.

Measurements of the temperature dependences $\Delta n_i(T)$ for both free and uniaxially loaded crystals showed that, in phase I, $\Delta n_i(T)$ varies almost linearly, while the transition to the incommensurate phase is accompanied by a change in slope. The PT to the ferroelectric phase at 458 K is characterized by a stepwise decrease $\delta(\Delta n_i) \approx -1.6 \times 10^{-4}$, whereas the PT at 439 K results in a stepwise increase $\delta(\Delta n_i) \approx \approx +3.0 \times 10^{-4}$.

The application of uniaxial stress does not alter the general shape of the $\Delta n_i(T)$ dependences. Differences appear only in the magnitudes of the temperature coefficients $d\Delta n_i/dT$ and the stepwise changes $\delta(\Delta n_i)$ during PTs: stress reduces $\delta(\Delta n_i)$ by an average of 0.2×10^{-4}.

The dispersion and temperature dependences of the piezooptic coefficients of $LiRbSO_4$ were studied. The coefficients show weak dispersion, $\frac{\partial\pi^0_{im}}{\partial\lambda} < 0$. In phase I, all coefficients slightly decrease in absolute value with increasing temperature, while the transition to phase II results in a stepwise decrease of approximately $\left|\delta\pi^0_{im}\right| \approx 1.20$ Br.

The contributions from the electrooptic and elastooptic effects, as well as from the order parameter, to the spontaneous changes in the piezooptic constant were estimated based on differences between the ferroelectric, ferroelastic, and incommensurate phases and the extrapolated data from the paraelec-

tric phase at room temperature. The dominant contribution (∼80%) occurs near T_4 and is caused by the emergence of spontaneous polarization, while further from this temperature, the contribution becomes negligible (10–15%).

The study was carried out within the framework of the state budget project "New broadband materials for detection and control of electromagnetic radiation in dual-purpose devices" (No. 0124U001228).

1. H. Mashiahama, K. Hasebe, K. Tanisaki. X-ray studies on successive structural transitions in $LiRbSO_4$. *J. Phys. Soc. Jap.* **47** (4), 1198 (1979).
2. H. Mashiahama, H.-G. Unruh. A new ferroelectric phase and a field induced phase of $LiRbSO_4$. *J. Phys. Soc. Jap.* **54** (2), 822 (1985).
3. W. Steurer, H. Wittmann, H. Jagodzinski. Phase transitions in $LiRbSO_4$. *Acta Cryst. B* **42**, 11 (1986).
4. A. Kunishige, H. Mashiyama. Crystalloptic study of phase transitions on $LiRbSO_4$. *J. Phys. Soc. Jap.* **56** (9), 3189 (1987).
5. C. Konak. Changes of optical properties at an incommensurate–commensurate phase transition in $(NH_4)_2BeF_4$ crystals. *J. Phys. Stat. Sol. (a)* **54**, 99 (1979).
6. C. Konak, J. Matras. Birefringente and electrooptical properties of $(NH_4)_2BeF_4$. *Czech. J. Phys. A* **26**, 577 (1976).
7. B.A. Strukov, P.S. Smirnov. The order of the commensurate–incommensurate phase transition in $(NH_4)_2BeF_4$ crystals. *Ferroelectrics* **66**, 85 (1986).
8. O.V. Bovgyra, V.I. Stadnyk, O.Z. Chyzh. Energy band structure and refractive properties of $LiRbSO_4$ crystals. *Phys. Solid State* **48** (7), 1268 (2006).
9. V.Y. Stadnyk, B.V. Andrievskii, L.T. Karplyuk, O.R. Onufriv. Band structure and birefringence of $LiRbSO_4$ crystals. *Opt. Spectrosc.* **121** (2), 283 (2016).
10. V.Yo. Stadnyk, M.O. Romanyuk. The baric changes of the electron polarizability of $LiRbSO_4$, $LiKSO_4$ and $(NH_4)_2BeF_4$ crystals. *Ferroelectrics* **317**, 63 (2005).
11. J.F. Nye. *Physical Properties of Crystals* (Clarendon Press, 1964).
12. N. Narasimhamurty. *Photoelastic and Electro-Optic Properties of Crystals* (Plenum Press, 1984).
13. A. Erba, R. Dovesi. Photoelasticity of crystals from theoretical simulations. *Phys. Rev. B* **88**, 045121 (2013).
14. P.P. Natali, L. Montalto, F. Davi, P. Mengucci, A. Ciriaco, N. Paone, D. Rinaldi. Theoretical and experimental evaluation of piezo-optic parameters and photoelastic constant in tetragonal PWO. *Appl. Opt.* **57**, 730 (2018).
15. B.G. Mytsyk, A.S. Andrushchak, D.M. Vynnyk, N.M. Demyanshyn, Ya.P. Kost, A.V. Kityk. Characterization of photoelastic materials by combined Mach–Zehnder and conoscopic interferometry: application to tetragonal lithium tetraborate crystals. *Opt. Laser Eng.* **127**, 105991 (2020).
16. R.F. Akhmedzhanov, M.I. Elboeva, S.Z. Mirzaev. Exploring of anisotropy of acousto-optic interaction in lead molybdate crystals. *Ultrasonics* **137**, 107203 (2024).
17. R.W. Dixon, M.G. Cohen. A new technique for measuring magnitudes of photoelastic tensors and its application to lithium niobite. *Appl. Phys. Lett.* **8**, 205 (1966).
18. R.W. Dixon. Photoelastic properties of selected materials and their relevance for applications to acoustic light modulators and scanners. *J. Appl. Phys.* **38**, 5149 (1967).
19. B.H. Myshchyk. *Photoelasticity of Anisotropic Materials* (Lira-Press, 2012) [ISBN: 978-966-397-144-8].
20. V.J. Stadnyk, M.O. Romanyuk. Piezooptic properties of $(NH_4)_2BeF_4$ crystals. *Phys. Status Solidi A* **158** (1), 289 (1996).
21. B. Mytsyk, V. Stadnyk, N. Demyanshyn, Ya. Kost, P. Shchepanskyi. Photoelasticity of ammonium sulfate crystals. *Opt. Mater.* **88**, 723 (2019).
22. M.O. Romanyuk. *Practicum in Crystaloptics and Crystalophysics* (Ivan Franko National University of Lviv, 2012) [ISBN 978-966-613-930-9].
23. M.O. Romanyuk. *Krystalooptyka* (Ivan Franko National University of Lviv, 2017) [ISBN: 978-617-10-0251-7].
24. V.I. Stadnyk, O.S. Kushnir, R.S. Brezvin, V.M. Gaba. Temperature and baric changes in the refractive indices of $LiKSO_4$ crystals. *Opt. Spectr.* **106** (4), 614 (2009).
25. A.U.A. Leitua, A. Rigni, A. Bourson, P. Pimenta. Optical study of $LiKSO_4$ crystals under uniaxially pressure. *Phys. Rev. B* **50** (5), 2754 (1994).
26. P.A. Shchepanskyi, V.M. Gaba, V.Yo. Stadnyk. The influence of partial isomorphic substitution on electronic and optical parameters of $ABSO_4$ group crystals. *Acta Phys. Pol. A* **133** (4), 819 (2018).
27. V.Yo. Stadnyk, N.A. Romanyuk, R.S. Brezvin. Refractometry of mechanically compressed $RbKSO_4$ crystals. *Crystallogr. Rep.* **50** (6), 961 (2005).
28. I.A. Pryshko, I.S. Novosad, Z.O. Kohut, V.M. Horina, O.M. Salapak. Dilatometric and refractive parameters of rubidium sulfate crystals at low temperatures. *Low Temp. Phys.* **50** (7), 584 (2024).
29. O.G. Vlokh, V.B. Kapustianik, I.I. Polovinko *et al.* Influence of domain structure on electro- and piezooptics properties of crystals. *Ferroelectrics* **111** (1), 333 (1990).
30. V. Kapustianik, Yu. Bazhan, Yu. Korchak. Crystalloptic properties of ferroic with the cation in the region of their phase transition. *Ukr. J. Phys. Opt.* **3** (4), 258 (2002).
31. L. Martynyuk-Lotocka, O. Mys, V. Adamiv *et al.* Elastic, piezooptical and acoustooptical properties of lithium tetraborate crystals. *Ukr. J. Phys. Opt.* **3** (4), 264 (2002).
32. I.P. Studeyak, M. Kranjec, M. Suslikov *et al.* Piezooptic effect in Cu_6PS_5Br crystals. *Opt. Spectr.* **93** (2), 300 (2002).

Received 01.12.25

В.В. Вишневський, І.А. Пришко,
В.Й. Стадник, О.А. Маркевич, З.О. Когут,
В.М. Салапак, І.С. Новосад

П'ЄЗООПТИЧНИЙ ЕФЕКТ У КРИСТАЛАХ $LiRbSO_4$

Синтезовано оптично якісний кристал $LiRbSO_4$ і досліджено вплив одновісного навантаження $\sigma_m \sim 200$ бар уздовж різних кристалофізичних напрямків на спектральні (300–700 нм) і температурні (77–650 K) залежності двопроменезаломлення Δn_i. Встановлено, що величина Δn_i досить чутлива до дії одновісних тисків і майже лінійно зростає зі зміною тиску, причому прикладання навантаження вздовж різних кристалофізичних напрямків спричиняє різні за знаком і величиною зміни $\delta\Delta n_i$, під час дії одновісного тиску $\sigma_Z = 77$ бар у кристалі індукується оптична псевдоізотропна точка, й одновісне навантаження не змінює характер залежностей $\Delta n_i(T)$. Відмінності виявлено лише у величинах стрибкоподібних змін Δn_i під час фазових переходів: одновісне навантаження зменшує величину $\delta(\Delta n_i)$. Досліджено дисперсійні й температурні залежності п'єзооптичних коефіцієнтів $\pi^0_{im}(\lambda)$ і $\pi^0_{im}(T)$ кристалів $LiRbSO_4$ і виявлено, що вони мають незначну дисперсію, так що $\partial\pi^0_{im}/\partial\lambda < 0$. Проаналізовано зміни $\pi^0_{im}(T)$ в околі точок фазових переходів. Оцінено внески електрооптичного й пружнооптичного ефектів і параметра порядку в спонтанні зміни п'єзооптичних коефіцієнтів і виявлено, що найбільший внесок (∼80%), зумовлений виникненням спонтанної поляризації, спостерігається в околі точки фазового переходу за температури T_4.

Ключові слова: кристал, двопроменезаломлення, дисперсія, одновісне навантаження, фазовий перехід, п'єзооптичні коефіцієнти.